EES Catalysis

PAPER

View Article Online
View Journal | View Issue

Cite this: *EES Catal.*, 2025, 3, 97

A supported Au/HZSM-5 catalyst for toluene removal by air plasma catalytic oxidation using the cycled storage-discharge (CSD) mode†

Amin Zhou,[a] Xiao-Song Li,*[a] Jing-Lin Liu,[a] Lan-Bo Di *[b] and Ai-Min Zhu [a]

Received 1st August 2024,
Accepted 2nd October 2024

DOI: 10.1039/d4ey00159a

rsc.li/eescatalysis

Air plasma catalytic oxidation of toluene (C_7H_8) with the cycled storage-discharge (CSD) mode is a promising technology for toluene (C_7H_8) removal. However, the problem of low CO_2 selectivity must be solved. In this work, a novel HZSM-5 (HZ) supported Au catalyst (Au/HZ) with *ca.* 5.7 nm Au nanoparticles was prepared by combining impregnation-ammonia washing and plasma treatment, and adopted for C_7H_8 removal. Au/HZ displays a large breakthrough capacity and an excellent oxidation ability of C_7H_8 in dry and wet air plasma. To investigate the mechanism of CO_2 selectivity improvement with the Au/HZ catalyst, air plasma catalytic oxidation of gaseous C_7H_8 and CO, as well as the adsorption of C_7H_8 and CO on the catalysts were conducted. For plasma-catalytic oxidation of gaseous C_7H_8 over Au/HZ, the CO_2 selectivity is 97.5%, significantly higher than those of HZ (55%) and Ag/HZ (62%). *In situ* TPD tests indicate that Au/HZ possesses a moderate adsorption strength for CO and C_7H_8 compared with HZ and Ag/HZ. Meanwhile, plasma oxidation of CO over Au/HZ reaches 100%, which is much higher than those of HZ (15%) and Ag/HZ (24%). Nearly 100% C_7H_8 conversion and CO_2 selectivity of plasma-catalytic oxidation of C_7H_8 on Au/HZ can be attributed to the moderate adsorption strength of Au/HZ for C_7H_8 and CO, and very high plasma catalytic activity for CO oxidation.

Broader context

The CO_2 selectivity and carbon balance have to be improved to ensure the long-term durability of the cycled storage-discharge (CSD) mode for removal of low-concentration volatile organic compounds, especially when using air plasma. Therefore, it is very necessary to combine a Au catalyst with a zeolite support as a two-in-one catalyst. However, it is difficult to obtain small-sized Au nanoparticles on non-reducible zeolites. Herein, a novel HZSM-5 (HZ) supported Au catalyst (Au/HZ) with *ca.* 5.7 nm Au nanoparticles was prepared by plasma treatment. The Au/HZ exhibits large breakthrough capacity and excellent oxidation ability for C_7H_8. *In situ* TPD tests indicate that Au/HZ possesses moderate adsorption strength for CO and C_7H_8 compared with HZ and Ag/HZ. Moreover, plasma oxidation of CO over Au/HZ reaches 100%. Therefore, both C_7H_8 conversion and CO_2 selectivity reach nearly 100% in air plasma for the Au/HZ catalysts. These findings underscore the outstanding toluene removal performance of the developed Au/HZ catalyst and its potential for air plasma catalytic oxidation of low-concentration VOC applications.

1. Introduction

Plasma catalytic oxidation is a facile and rapid technology for removal of volatile organic compounds (VOCs) at low temperature.[1] For removal of low-concentration VOCs, normal continuous operation of the plasma catalytic process leads to high energy cost and generation of secondary pollutants like O_3 and NO_x.[2,3] To address this issue, a cycled storage-discharge (CSD) mode of plasma catalysis was proposed.[4–6] The CSD mode involves two stages: VOCs are firstly adsorbed onto the catalysts till saturation in the storage stage (plasma off), and then the adsorbed VOCs are oxidized to CO_2 and H_2O in the discharge stage (plasma on). The transient discharge time significantly reduces energy consumption and production of secondary pollutants, making it a promising technology for removal of VOCs.[5,7]

Due to the unique pore structure and large VOC storage capacity, molecular sieves are widely adopted for removal of VOCs using the CSD mode.[8–10] Among the molecular sieves, HZSM-5 (HZ) with high silica to alumina ratios is more attractive due to its large storage capacity, good hydrophobicity

[a] *Laboratory of Plasma Physical Chemistry, Dalian University of Technology, Dalian 116024, China. E-mail: lixsong@dlut.edu.cn*
[b] *College of Physical Science and Technology, Dalian University, Dalian 116622, China. E-mail: dilanbo@163.com*

† Electronic supplementary information (ESI) available. See DOI: https://doi.org/10.1039/d4ey00159a

and stability.[11] Confined to the low CO_2 selectivity and carbon balance of HZ, HZ supported Ag, Cu, Mn, or Ce catalysts have been prepared and employed for plasma catalytic oxidation of benzene,[7,12] toluene (C_7H_8)[13,14] and formaldehyde (HCHO).[5] These catalysts exhibited large storage capacity and high plasma catalytic oxidation activity for removal of VOCs. However, oxygen plasma is generally adopted, which is not economically affordable and inconvenient. Meanwhile, the CO_2 selectivity and carbon balance need to be further improved to ensure the long-term durability of the CSD mode, especially when using air plasma.

Since Au catalysts are active for CO oxidation at low temperature,[15] our previous work employed the tandem effect of in-plasma zeolite and a post-plasma Au/TiO_2 catalyst for complete oxidation of C_7H_8 to CO_2, and nearly 100% CO_2 selectivity at 100% C_7H_8 conversion was obtained.[16] To make it more convenient and beneficial for practical applications, it is very necessary to combine Au with the HZ support to prepare a Au/HZ catalyst. However, the activity of Au catalysts is sensitive to Au particle size, and larger particle sizes are generally less active.[17] In order to obtain small Au nanoparticles, reducible oxides[18] (such as TiO_2, CeO_2, *etc.*) are generally used as supports by using a deposition–precipitation method. Differently, zeolites such as HZ are non-reducible supports, and Au nanoparticles generally possess large size.[15,19] Therefore, so far Au/HZ has not been reported in plasma catalytic removal of VOCs.

Plasma has been proved to be an efficient method for synthesizing supported metal catalysts.[20,21] Herein, a Au/HZ catalyst was prepared by combining impregnation-ammonia washing and plasma treatment, and applied for air plasma catalytic removal of C_7H_8. Au/HZ displays large breakthrough capacity, excellent oxidation activity, and stability for C_7H_8 removal. To obtain insight into the underlying mechanism of the excellent performance of Au/HZ, plasma oxidation of gaseous C_7H_8 and CO was performed, and *in situ* TPD tests were adopted to further investigate C_7H_8 and CO adsorption on the catalysts. The results indicate that the nearly 100% CO_2 selectivity of the plasma-catalytic oxidation of C_7H_8 on Au/HZ can be attributed to the moderate adsorption strength of Au/HZ for C_7H_8 and CO, and very high plasma catalytic activity for CO oxidation.

2. Experimental

2.1 Preparation of catalysts

HZ supported Au catalysts were prepared by a combination of impregnation-ammonia washing and plasma treatment using $HAuCl_4$ as the Au precursor. Prior to the preparation, HZ was calcined in a muffle furnace at 550 °C for 3 h and then cooled to room temperature. Then, 1 g of HZ powder was immersed in 2.2 mL of $HAuCl_4$ solution and left at room temperature in the dark for 12 h. Subsequently, it was washed twice with ammonia water (pH = 12) and deionized water to remove the chloride ions. The obtained sample was centrifuged, dried at 80 °C for 6 h, prepared into tablets, crushed, and sieved to a size of 40–60 mesh. Finally, the sample was treated by air plasma (with an input power of 7.0 W and an air flow rate of 100 mL min^{-1}) using a coaxial dielectric barrier discharge (DBD) reactor for 20 min to obtain the Au/HZ catalysts. An AC high voltage power supply (CTP-2000 K, Nanjing Suman, China) was used to ignite the plasma. Details of the DBD reactor can be found in our previous work.[22] The loading amounts of Au in the Au/HZ catalysts are 0.3 wt%, 0.6 wt% and 1.1 wt%, respectively. Additionally, in comparison with plasma treatment, a Au/HZ catalyst was also prepared by thermal treatment at 200 °C in air atmosphere for 2 h. Unless otherwise specified, the Au loading in Au/HZ is 0.6 wt%.

Since Ag/HZ is generally adopted for removal of VOCs by thermal catalysis and plasma catalysis, a Ag/HZ catalyst was also prepared by an incipient-wetness impregnation method using $AgNO_3$ and HZ as the Ag precursor and support, respectively, according to previous work.[23] 1 g of HZ powder was immersed in a certain concentration of $AgNO_3$ solution and left at room temperature in the dark for 12 h. It was then dried at 110 °C for 3 h and calcined in a muffle furnace at 450 °C for 3 h. Finally, the prepared Ag/HZ powder was prepared into tablets, crushed, and sieved to a size of 40–60 mesh for use.

2.2 Adsorption and plasma oxidation of C_7H_8

The breakthrough capacity of the catalysts for C_7H_8 is defined as the adsorption capacity from the beginning of C_7H_8 adsorption to the time when the concentration at the outlet of the reaction tube reaches 5% of the initial concentration of C_7H_8. The determination of the initial C_7H_8 concentration and the reaction evaluation setup are reported in our previous work.[22] The initial concentration of C_7H_8 is *ca.* 105 ppm.

Simulated air plasma was adopted for C_7H_8 removal using the cycled storage-discharge (CSD) mode. First, simulated air containing C_7H_8 was introduced into the same DBD reactor as that used for the preparation of catalysts. After adsorption for a certain period, simulated air was used to purge the catalyst bed to remove weakly adsorbed C_7H_8. Subsequently, the CTP-2000 K plasma power supply was turned on to treat the adsorbed C_7H_8 using simulated air as the working gas with an input power (P_{in}) of 7.0 W and a discharge power (P_{dis}) of 1.5 W. P_{in} was determined using a wattmeter, and P_{dis} was obtained by the Lissajous figure method using a 0.47 μF capacitance. The discharge time in this work was 20 min. Gaseous products were monitored online by using a nondispersive infrared gas analyzer (S710, Sick-Maihak, Germany) and a mass spectrometer (HPR-20 QIC, Hiden Analytical, UK).

Plasma catalytic oxidation of adsorbed C_7H_8 was conducted over the Au/HZ catalysts prepared by thermal treatment and air plasma treatment, respectively. It was found that the plasma-activated Au/HZ catalyst can show higher CO_2 selectivity (Fig. S1, ESI†). Therefore, unless otherwise specified, the Au/HZ catalysts are prepared by air plasma treatment.

To understand the underlying mechanism of the catalysts for oxidation of adsorbed C_7H_8, plasma-catalytic oxidation of gaseous C_7H_8 and CO was also performed. Simulated air

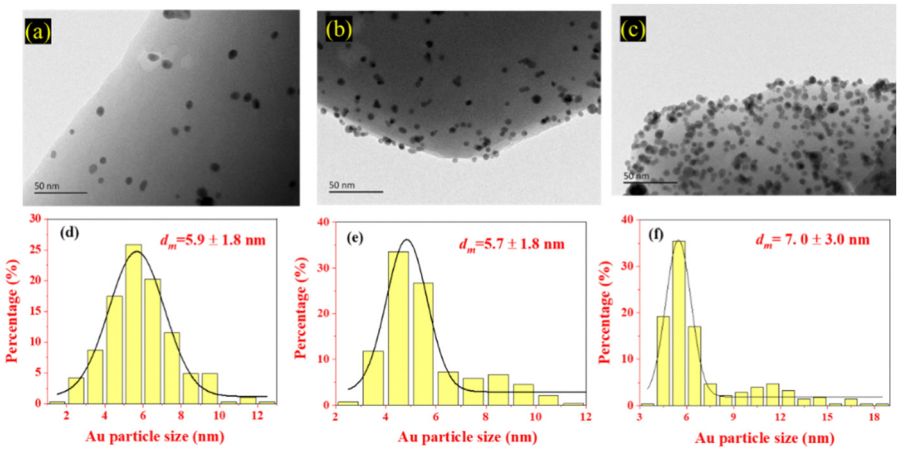

Fig. 1 TEM images of Au/HZ with different Au loadings: (a) 0.3 wt%, (b) 0.6 wt%, and (c) 1.1 wt%, and (d)–(f) the corresponding size distribution histograms of Au nanoparticles.

containing certain concentrations of C_7H_8 or CO was introduced into the DBD reactor with a 7.0 W input power.

3. Results and discussion

3.1 Valence state and particle size of Au in Au/HZ catalysts

To overcome the problem of large size of Au nanoparticles on HZ prepared by the conventional deposition–precipitation method, Au/HZ catalysts were prepared using an impregnation-ammonia washing combined with the plasma treatment method. TEM images of Au/HZ with different Au loadings were recorded and are shown in Fig. 1(a)–(c). The Au nanoparticles were uniformly distributed in the Au/HZ samples. By calculating more than 300 Au nanoparticles, the particle size distribution histograms of Au were obtained, as shown in Fig. 1(d)–(f). The statistical analysis reveals an average size of 5.7–5.9 nm, when the Au loading is below 0.6 wt%. With increasing Au loading to 1.1 wt%, the average size slightly increases to 7.0 nm due to enhanced aggregation and growth of Au nanoparticles. Notably, the method used in this work yields smaller Au nanoparticles compared to the literature (Au loading of 0.5 wt%, average size of 8.1 ± 2.4 nm).[24]

To investigate the valence state of Au, the Au/HZ catalyst (0.6 wt% Au) was analyzed using XPS and H_2-TPR. As shown in Fig. 2(a), the XPS results indicate that Au species primarily exist as Au^0 and $Au^{\delta+}$ in Au/HZ, with the proportion of Au^0 (~55 at%) slightly exceeding that of $Au^{\delta+}$. The UV-vis diffuse reflectance spectroscopy (DRS) characterization of Au/HZ (Fig. S2, ESI†) displays a distinct absorption peak at 560 nm, which can be attributed to the plasmonic resonance absorption of Au^0. This confirms the presence of Au^0 in Au/HZ, which is consistent with the XPS results. The H_2-TPR analysis of the Au/HZ catalyst (Fig. 2(b)) reveals a hydrogen consumption peak at 98 °C associated with the reduction of $Au^{\delta+}$. Furthermore, a CO-TPR experiment was conducted on the Au/HZ catalyst, under a 1400 ppm CO/He atmosphere, resulting in concentration change curves of CO and CO_2 during the CO-TPR process, along with the corresponding mass spectrometry signals, as shown in Fig. 2(c) and (d). The CO reduction peak, observed at around 100 °C and shown in Fig. 2(c) for the Au/HZ catalyst, is attributed to the reduction of $Au^{\delta+}$ species, consistent with the H_2-TPR results. At 630 °C, the concentration of CO (m/z = 28) decreases, accompanied by a peak in CO_2 generation. The gaseous products detected include CO_2 (m/z = 44) and H_2 (m/z = 2) (Fig. 2(d)).

This indicates the occurrence of the water–gas shift reaction ($CO + H_2O \rightarrow CO_2 + H_2$) as the temperature rises, involving the reaction of CO with adsorbed H_2O molecules on the catalyst surface.

3.2 Breakthrough capacity of Au/HZ catalysts for C_7H_8

The breakthrough capacity of Au/HZ for C_7H_8 with different Au loadings is shown in Fig. 3(a). With increasing the Au loading, the C_7H_8 breakthrough capacity first increases and then decreases. Under both dry and wet conditions, the C_7H_8 breakthrough capacity of the Au/HZ catalysts reaches the maximum at a 0.6 wt% Au loading. Moreover, Au/HZ catalysts exhibit very close C_7H_8 breakthrough capacities under dry and wet conditions, indicating their good moisture resistance. In addition, Au/HZ demonstrates a significantly larger C_7H_8 breakthrough capacity than HZ and comparable performance to Ag/HZ (Fig. S3, ESI†).

The C_7H_8 breakthrough capacity of Au/HZ is significantly improved in comparison with HZ. TPD technology was applied to analyze C_7H_8 adsorption sites on HZ and Au/HZ for exploring the mechanism of increased C_7H_8 breakthrough capacity. With the same adsorption amount of C_7H_8, Au/HZ catalysts with different Au loadings were subjected to TPD experiments under an Ar atmosphere, and the corresponding C_7H_8 TPD curves were obtained, as shown in Fig. 3(b)–(d). Two C_7H_8 desorption peaks appear on Au/HZ with different Au loadings. Combined with the C_7H_8 TPD curve on HZ, the C_7H_8 desorption peak at around 200 °C is attributed to C_7H_8 adsorbed on the HZ adsorption site, while the peak at around 300 °C is ascribed to C_7H_8 adsorbed on Au adsorption sites. With increasing Au

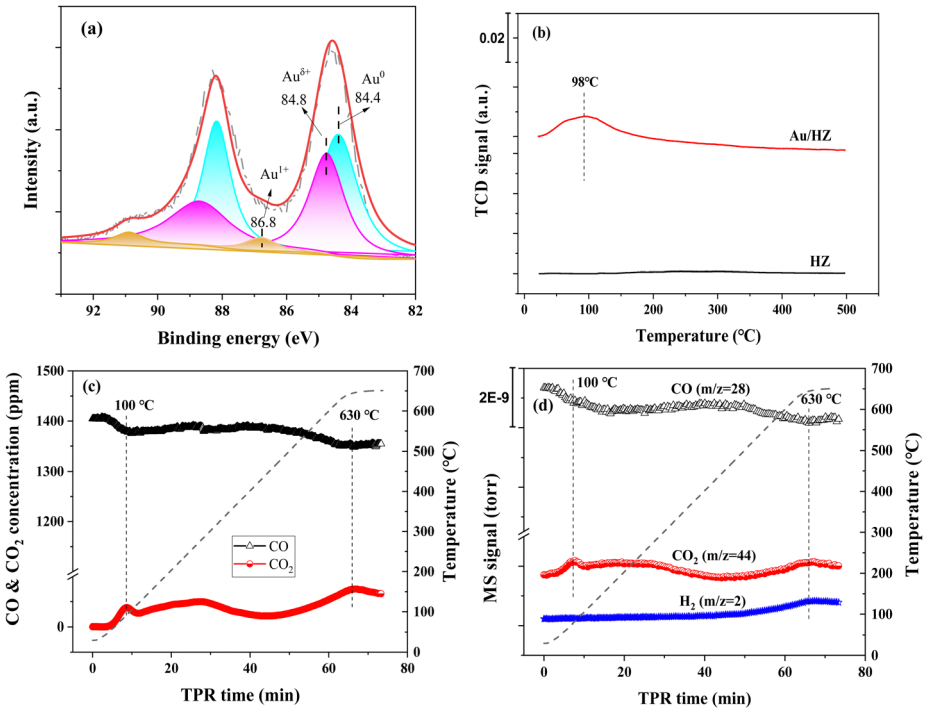

Fig. 2 (a) XPS spectrum of Au 4f in Au/HZ; (b) H_2-TPR profiles of Au/HZ and HZ; and (c) CO and CO_2 concentrations and (d) MS signals of CO, CO_2 and H_2 in CO-TPR tests over Au/HZ (0.6 wt% Au). H_2-TPR conditions: 30 mL min^{-1} of 5% H_2/Ar, 0.20 g Au/HZ. CO-TPR conditions: 100 mL min^{-1} of 1400 ppm CO/He.

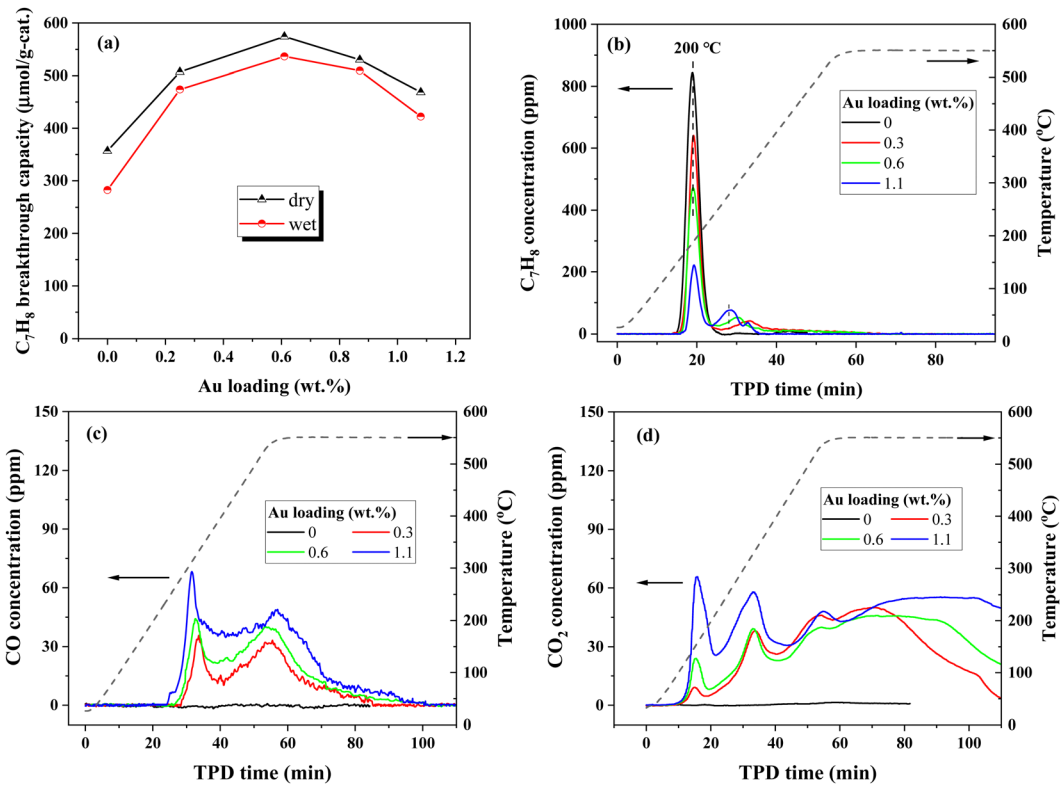

Fig. 3 Effect of Au loading on (a) C_7H_8 breakthrough capacity under dry and wet conditions; (b) C_7H_8 concentration, (c) CO concentration, and (d) CO_2 concentration in TPD tests. Adsorption conditions: 100 mL min^{-1} of dry or wet (RH = 66%, 20 °C) simulated air with C_7H_8; TPD conditions: $n^0_{C_7H_8} = 13.5$ μmol, 100 mL min^{-1} of Ar.

loading, the C_7H_8 concentration desorbed from HZ adsorption sites gradually decreased, while the C_7H_8 concentration desorbed from Au adsorption sites increased, indicating an enhanced adsorption strength of Au/HZ catalysts for C_7H_8 with increasing Au loading. Meanwhile, the amounts of CO and CO_2 generated from oxidation of adsorbed C_7H_8 on Au adsorption sites also increased with increasing Au loading.

3.3 Performance of plasma catalytic oxidation of adsorbed C_7H_8 on Au/HZ catalysts

From Fig. 3, it can be seen that Au loading exhibits a significant impact on the C_7H_8 breakthrough capacity and adsorption strength of Au/HZ. The effect of Au loading on plasma-catalytic oxidation of C_7H_8 using Au/HZ was further investigated and is illustrated in Fig. 4. As shown in Fig. 4(a), Au/HZ significantly reduces CO production during the discharge stage under both dry C_7H_8 storage and simulated air discharge conditions compared with HZ. From Fig. 4(b) and (c), it can be observed that with Au loading increasing from 0 to 0.6 wt%, CO_2 production increases from 100.4 to 150.3 μmol, while CO production decreases from 65.4 to 15.4 μmol. Correspondingly, CO_2 selectivity increases from 57% to 86%, and CO selectivity decreases from 33% to 8%. However, when Au loading increases to 0.9 wt% and 1.1 wt%, CO_2 and CO produced remain almost unchanged. The corresponding CO selectivity decreases from 33% of HZ to around 10%, and the CO_2 selectivity remains at approximately 75%. The adsorption of C_7H_8 and intermediates on Au/HZ strengthens as the Au loading increases (Fig. 3(b)–(d)), and some active sites may be occupied by intermediates, thus affecting further oxidation of C_7H_8 and leading to a decrease in CO_x production during the discharge process. Additionally, when the Au loading increases to 1.1 wt%, an increased size of Au nanoparticles reduces the plasma-catalytic activity. Therefore, appropriate Au loading for Au/HZ catalysts is 0.6 wt% at both storage and discharge stages in this work.

According to the CO_x selectivity results (the sum of CO and CO_2 sensitivities) from Fig. 4(c), CO_x selectivity during the discharge process reaches about 90%, indicating that small amounts of intermediates are adsorbed on the catalysts or desorbed into the gas phase during the discharge process. To verify the carbon balance results of the Au/HZ catalysts, an *in situ* TPO test was conducted on the Au/HZ catalysts under a 10% O_2/Ar atmosphere after three cycles of storage and discharge (Fig. S4, ESI†). Intermediates adsorbed on the catalysts are fully oxidized to CO_2, and the amount of intermediates can be determined through the CO_2 production, thus obtaining carbon balance results. The CO_2 concentrations during the TPO process are shown in Fig. S4(a) (ESI†). Compared to one desorption peak of CO_2 on HZ, two CO_2 desorption peaks appear on the Au/HZ catalysts, with significantly increased peak values and areas. This indicates that there are two types of surface intermediates absorbed on the Au/HZ catalysts after discharge, which are gradually oxidized to CO_2 during the TPO process. With the further increase of Au loading to more than

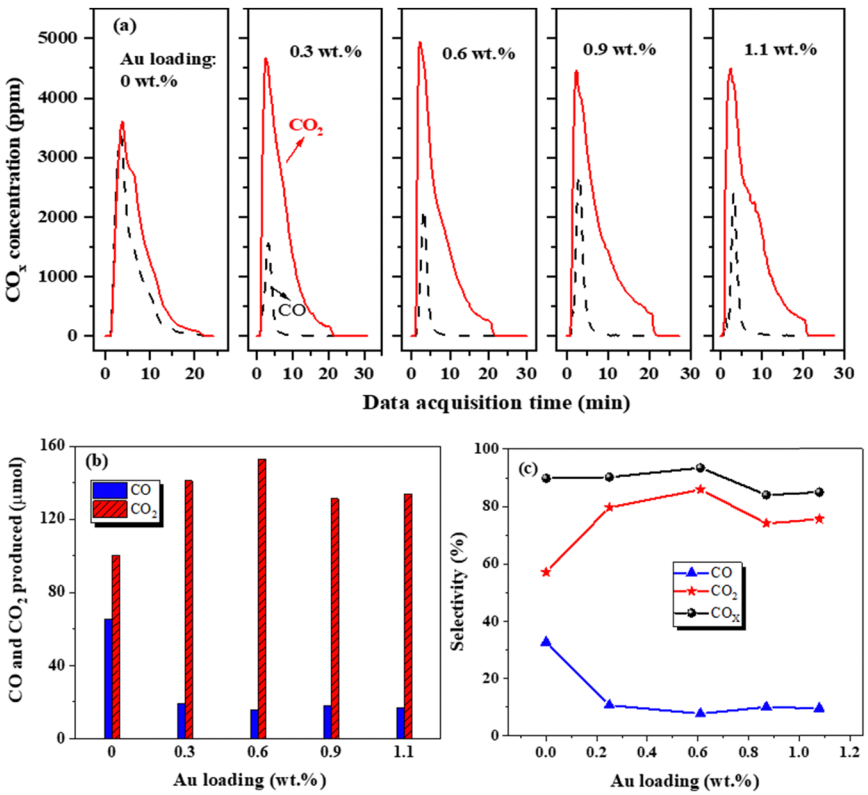

Fig. 4 Effect of Au loading on (a) CO_x concentration, (b) the amount of CO_x produced, and (c) CO_x selectivities in plasma oxidation of adsorbed C_7H_8 on Au/HZ. Conditions: $n^0_{C_7H_8}$ = 25.2 μmol, P_{in} = 7.0 W, t_{dis} = 20 min, 100 mL min^{-1} of dry simulated air.

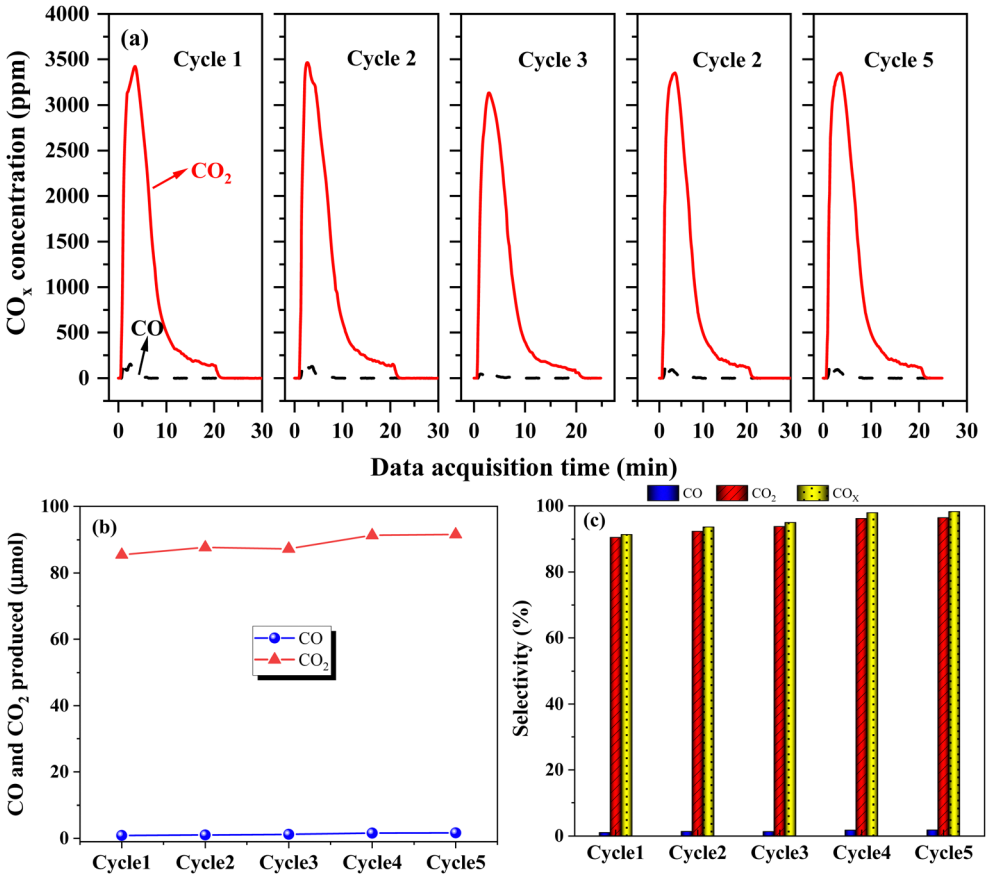

Fig. 5 (a) CO_x concentration, (b) amounts of CO and CO_2 produced, and (c) CO, CO_2, and CO_x selectivities of five cycles of C_7H_8 CSD oxidation over the Au/HZ catalyst. Conditions: $n^0_{C_7H_8}$ = 13.5 μmol, P_{in} = 7.0 W, t_{dis} = 20 min, 100 mL min^{-1} of dry simulated air.

0.6 wt%, the peak surface values of CO_2 concentration basically no longer increase.

CO_2 produced from surface intermediates on the Au/HZ catalysts with different Au loadings can be obtained by integrating the CO_2 concentration-time curve, hence obtaining the carbon balance (average of three cycles), as shown in Fig. S4(b) (ESI†). The carbon balance of 0.6 wt% Au/HZ reaches 97.5%. It is higher than that of HZ (carbon balance of 93%) due to the stronger adsorption strength of Au/HZ for C_7H_8, which may reduce desorption during the discharge process. This is consistent with the infrared spectroscopy result that no desorbed C_7H_8 or intermediates are detected during the discharge process.

To evaluate the oxidation performance and stability of Au/HZ in the CSD experiments, five cycles of C_7H_8 storage-discharge oxidation were conducted. The corresponding CO_x production and selectivity results are shown in Fig. 5. Compared to the CO_2 production, CO production is negligible. CO_2 selectivity reached approximately 95% in 5 cycles. This indicates that the Au/HZ catalyst exhibits stable and excellent plasma-catalytic oxidation performance for C_7H_8.

To obtain insight into the underlying mechanism of the excellent performance of the Au/HZ catalysts for complete oxidation of C_7H_8, at first, plasma-catalytic oxidation of gaseous C_7H_8 and CO was conducted in comparison to HZ and the widely adopted Ag/HZ catalyst. CO and CO_2 concentrations as a function of discharge time over the catalysts for gaseous C_7H_8 oxidation are shown in Fig. 6(a)–(c). 100% C_7H_8 conversion is obtained on the catalysts. No CO is detected on Au/HZ, and the CO_2 concentration on Au/HZ is significantly higher than those on Ag/HZ and HZ. In contrast, both HZ and Ag/HZ produce a significant amount of CO during plasma-catalytic oxidation of C_7H_8, with CO_2 concentration on Ag/HZ being slightly higher than that on HZ. Accordingly, CO and CO_2 selectivity for plasma-catalytic oxidation of C_7H_8 over different catalysts are shown in Fig. 6(d). The CO_2 selectivity over HZ and Ag/HZ is 55% and 62%, respectively, while it reaches as high as 97.5% over Au/HZ.

Plasma-catalytic oxidation of CO was also conducted in comparison with the HZ and Ag/HZ catalysts, as shown in Fig. 7. It can be noted that the Au/HZ catalyst has no activity for thermal catalytic oxidation of CO at room temperature. Even at 100 °C, the Au/HZ catalyst only exhibits a CO conversion of approximately 5%, being slightly higher than that of Ag/HZ (~3%), while HZ shows no thermal catalytic activity (Fig. S5, ESI†). In contrast, the Au/HZ catalyst is distinguished from HZ and Ag/HZ catalysts for plasma-catalytic CO oxidation. As shown in Fig. 7(a)–(c), only a small amount of

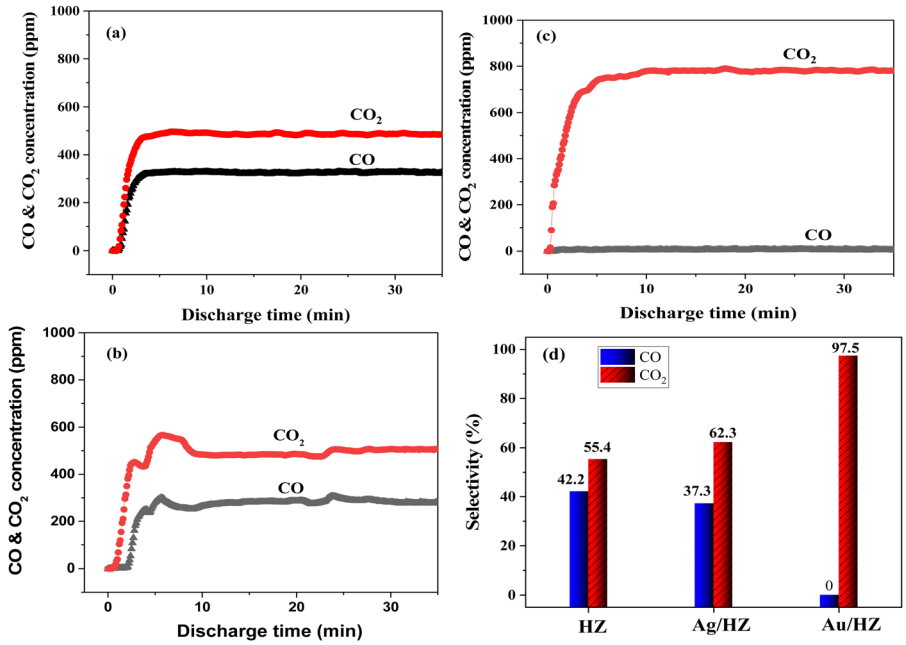

Fig. 6 CO and CO_2 concentrations of gaseous C_7H_8 oxidation in dry simulated air plasma over (a) HZ, (b) Ag/HZ (1.2 wt% Ag), and (c) Au/HZ (0.6 wt% Au), and (d) their corresponding CO_x selectivities. Conditions: 100 mL min^{-1} of simulated air with 115 ppm C_7H_8, P_{in} = 7.0 W.

CO is converted to CO_2 on the HZ and Ag/HZ catalysts, resulting in around 240 and 365 ppm outlet CO_2 concentrations, respectively. Notably, no CO is detected in the outlet gas for the Au/HZ catalyst. That is, CO is fully oxidized to CO_2 on Au/HZ under the plasma. The CO conversion of different catalysts is presented in Fig. 7(d). Ag/HZ shows a slightly higher CO conversion (24%) compared to HZ (15%), while Au/HZ achieves complete CO conversion (100%). This is well consistent with the CO_2 selectivity obtained in plasma-catalytic oxidation of C_7H_8, suggesting that enhanced CO_2 selectivity of Au/HZ in C_7H_8 oxidation is correlated with its good CO oxidation activity in plasma.

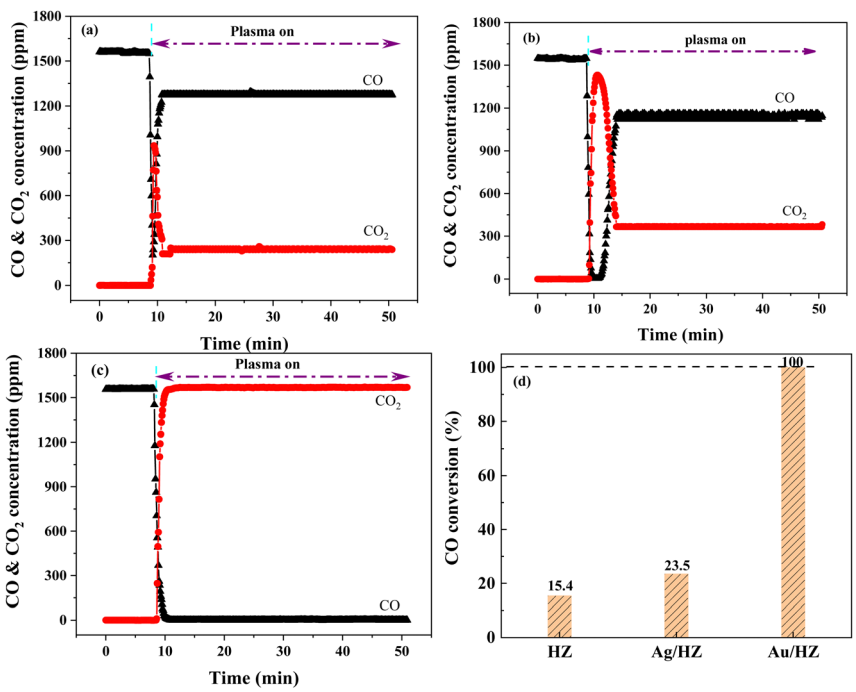

Fig. 7 CO and CO_2 concentrations of CO oxidation in dry simulated air plasma over (a) HZ, (b) Ag/HZ (1.2 wt% Ag), and (c) Au/HZ (0.6 wt% Au), and (d) the corresponding CO conversion over different catalysts. Conditions: 100 mL min^{-1} of simulated air with 1555 ppm CO, m_{cat} = 0.20 g, P_{in} = 7.0 W.

To further investigate C_7H_8 and CO adsorption on the HZ, Ag/HZ, and Au/HZ catalysts, TPD tests of the catalysts were carried out. First, TPD experiments on the HZ, Ag/HZ, and Au/HZ catalysts with identical amounts of adsorbed C_7H_8 were conducted, as shown in Fig. 8(a). C_7H_8 desorption on HZ occurs at approximately 200 °C. In contrast, Ag/HZ and Au/HZ display two distinct desorption peaks for C_7H_8. Apart from the peak near 200 °C attributed to C_7H_8 adsorption on the HZ sites, additional desorption peaks at around 300 and 440 °C, respectively, are observed for Ag and Au adsorption sites. The C_7H_8 desorption temperatures suggest the adsorption strength of the catalysts for C_7H_8 follows the order: HZ < Au/HZ < Ag/HZ.

Then CO-TPD tests of the HZ, Ag/HZ, and Au/HZ catalysts were also carried out. Simulated air containing CO was passed through the catalyst bed for 5 min of adsorption, followed by 10 min of Ar purging. Subsequently, the catalyst bed was heated from room temperature to 550 °C (at a ramp rate of 10 °C min^{-1}) under an Ar atmosphere. The CO-TPD curves for the HZ, Ag/HZ, and Au/HZ catalysts are shown in Fig. 8(b). A distinct CO desorption peak is observed on Ag/HZ, while nearly no CO desorption peak is detected on HZ. Differently, Au/HZ exhibits a small amount of CO_2 desorption, coming from CO oxidation on Au/HZ during the TPD process. In other words, Au/HZ demonstrates moderate CO adsorption, and Ag/HZ displays a stronger CO adsorption ability than Au/HZ and HZ. Furthermore, *in situ* DRIFT was performed to investigate the adsorption process of CO on HZ, Ag/HZ, and Au/HZ, as shown in Fig. 8(c). The CO adsorption peaks on Au/HZ are observed at 2115 and 2172 cm^{-1}, which are close to the positions on HZ (2116 and 2172 cm^{-1}). Since the CO adsorption on HZ and Au/HZ is weak, the adsorption peak on them is close to the infrared spectra of gaseous CO (located at 2120 and 2173 cm^{-1}, respectively, with symmetrical peak shapes). With increasing the adsorption time, the intensity of the CO adsorption peak on HZ changes slightly, with a slight increase in the vibration peak at 2172 cm^{-1}. In contrast, the CO adsorption peaks at 2115 and 2172 cm^{-1} on Au/HZ show a certain increase, attributed to the reduction of a small amount of $Au^{\delta+}$ species to Au^0 by CO.[25,26] This is consistent with the XPS and UV-vis DRS characterization results of Au/HZ. In contrast, CO adsorption on Ag/HZ is much stronger than those on HZ and Au/HZ (with an intensity difference of nearly two orders of magnitude), with an obvious blue shift. Due to the strong adsorption of CO by Ag/HZ, the intensity of the vibrational spectral peak of CO located at 2177 cm^{-1} (Ag adsorption site) is much larger than that of the peak at 2122 cm^{-1} (HZ adsorption site). In conclusion, the Au/HZ catalyst exerts a moderate adsorption effect on CO, which is important for the plasma-catalytic oxidation of C_7H_8 and CO.

In summary, TPD experiments of C_7H_8 and CO adsorption on the HZ, Ag/HZ, and Au/HZ catalysts indicate that Au/HZ shows a moderate adsorption effect on C_7H_8 and CO. As for plasma-catalytic oxidation of adsorbed C_7H_8, catalysts with excessively strong adsorption may lead to prolonged occupation of active sites, resulting in incomplete C_7H_8 oxidation and lower CO_2 selectivity. Conversely, catalysts with weak adsorption may cause partial desorption of C_7H_8 during the discharge process, leading to decreased CO_2 selectivity and carbon balance. Compared to HZ and Ag/HZ, Au/HZ exhibits a moderate adsorption strength for C_7H_8 and CO, which contributes significantly to its superior performance in plasma-catalytic oxidation of C_7H_8.

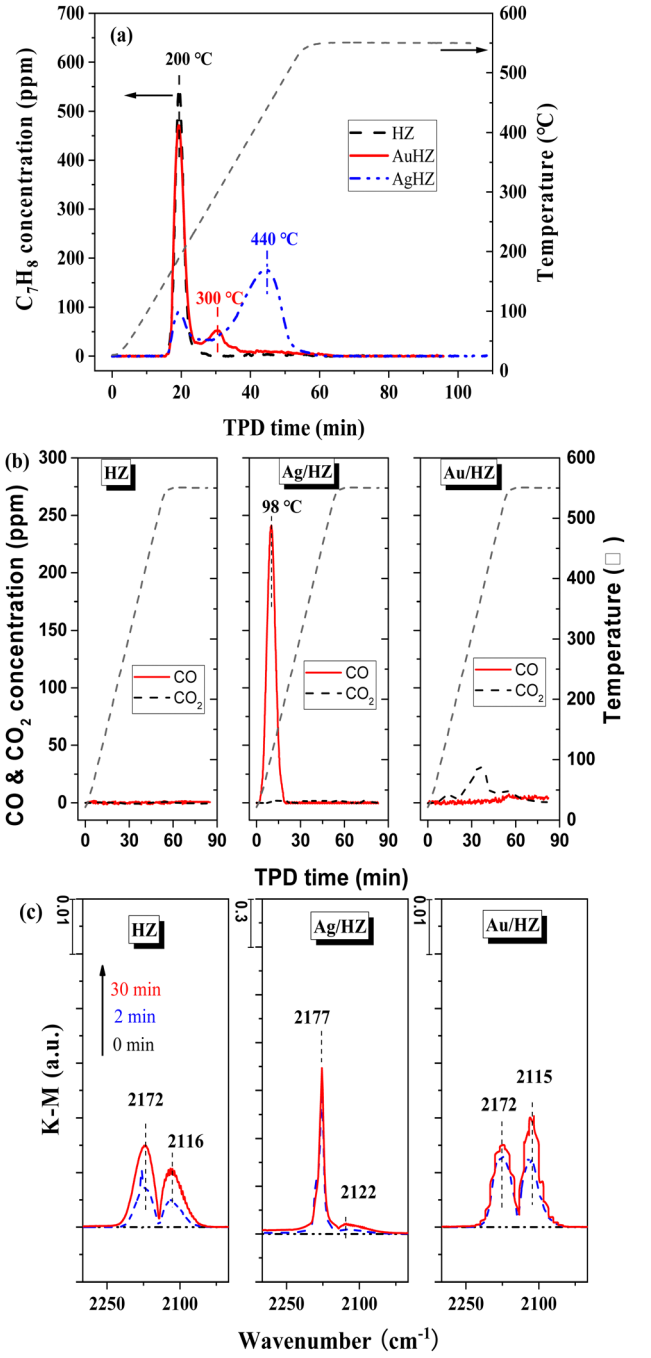

Fig. 8 C_7H_8 desorption over HZ, Ag/HZ and Au/HZ: (a) C_7H_8 concentrations in TPD tests; TPD conditions: $n^0_{C_7H_8}$ = 13.5 μmol, 100 mL min^{-1} of Ar. C_7H_8 adsorption conditions: 100 mL min^{-1} of C_7H_8/N_2, 25 °C. (b) CO and CO_2 concentrations during the CO-TPD process over HZ, Ag/HZ (1.2 wt% Ag) and Au/HZ (0.6 wt% Au). TPD conditions: 100 mL min^{-1} of Ar, 10 °C min^{-1}. (c) *In situ* DRIFT spectra of CO adsorption over HZ, Ag/HZ and Au/HZ. CO adsorption conditions: 40 mL min^{-1} of 5% CO/He, 25 °C.

4. Conclusion

A novel Au/HZ catalyst, prepared by impregnation combined with plasma treatment, exhibits excellent performance for C_7H_8 removal by air plasma catalytic oxidation using the cycled storage-discharge (CSD) mode. The size of Au is *ca.* 5.7 nm in Au/HZ (0.6 wt%), and the Au species are mainly in the form of Au^0 and $Au^{\delta+}$. Au/HZ possesses a large C_7H_8 breakthrough capacity, which is significantly higher than that of HZ. For plasma-catalytic oxidation of gaseous C_7H_8 over Au/HZ, the CO_2 selectivity is 97.5%, significantly higher than those of HZ (55%) and Ag/HZ (62%). This suggests that Au/HZ is indeed an excellent catalyst in air plasma catalytic oxidation of C_7H_8, especially suitable for the cycled storage-discharge mode. *In situ* TPD tests show that Au/HZ exhibits a moderate adsorption strength for C_7H_8 and CO, compared with HZ and Ag/HZ. Moreover, Au/HZ exhibits 100% CO conversion during plasma catalytic CO oxidation, which is much higher than those of HZ (15%) and Ag/HZ (24%). Therefore, the nearly 100% CO_2 selectivity of the plasma-catalytic oxidation of C_7H_8 on Au/HZ can be attributed to the moderate adsorption strength of Au/HZ for C_7H_8 and CO, and very high plasma catalytic activity for CO oxidation.

Author contributions

A. Z.: investigation, methodology, data curation, formal analysis, writing – original draft. X. L.: conceptualization, formal analysis, investigation, methodology, investigation, writing – review & editing. J. L.: investigation, methodology, data curation. L. D.: investigation, methodology, funding acquisition, conceptualization, writing – review & editing. A. Z.: conceptualization, formal analysis, funding acquisition, methodology, writing – review & editing.

Data availability

The data supporting this article have been included as part of the ESI.†

Conflicts of interest

There are no conflicts to declare.

Acknowledgements

This work was supported by the National Natural Science Foundation of China (Grant No. 11975069 and 52077024) and Xingliao Talents Program (Grant No. 2022RJ16 and XLYC2203147).

References

1 Y. Mu and P. T. Williams, *Chemosphere*, 2022, **308**, 136481.
2 S. Sharmin, V. Arne, L. Christophe, D. G. Nathalie and M. Rino, *Catalysts*, 2015, **5**(2), 718–746.
3 M. Schiavon, V. Torretta, A. Casazza and M. Ragazzi, *Water, Air, Soil Pollut.*, 2017, **228**(10), 388.
4 A. O. Hyun-Ha Kim and Shigeru Futamura, *Appl. Catal., B*, 2008, **79**(4), 356–367.
5 D. Z. Zhao, X. S. Li, C. Shi, H. Y. Fan and A. M. Zhu, *Chem. Eng. Sci.*, 2011, **66**(17), 3922–3929.
6 D. I. Ogata Atsushi, Koichi Mizuno, Satoshi Kushiyama and Toshiaki Yamamoto, *IEEE Trans. Ind. Appl.*, 2001, **37**(4), 959–964.
7 H. Y. Fan, X.-S. Li, D. Z. Zhao, Y. Xu and A. M. Zhu, *J. Phys. D: Appl. Phys.*, 2009, **42**(22), 225105.
8 K. J. Kim and H. G. Ahn, *Microporous Mesoporous Mater.*, 2012, **152**, 78–83.
9 Q. H. Trinh, M. S. Gandhi and Y. S. Mok, *Jpn. J. Appl. Phys.*, 2014, **54**, 01AG04.
10 J. E. Lee, Y. S. Ok, D. C. W. Tsang, J. H. Song and Y. K. Park, *Sci. Total Environ*, 2020, **719**, 137405.
11 Y. Liu, X. S. Li, J. L. Liu, J. L. Wu, D. Ye and A. M. Zhu, *Catal. Sci. Technol.*, 2016, **6**(11), 3788–3796.
12 H. A. M. Mohammad Sharif Hosseini and Rasoul Yarahmadi, *Plasma Chem. Plasma Process.*, 2018, **39**, 125–142.
13 H. Y. Fan, X. S. Li, Y. Liu, J. Liu and A. M. Zhu, *CIESC J.*, 2011, **62**(7), 1922–1926.
14 W. Z. Wang, H. Wang, T. L. Zhu and X. Fan, *J. Hazard. Mater.*, 2015, **292**(15), 70–78.
15 J. Cao, R. J. Lewis, G. Qi, D. Bethell, M. J. Howard, B. Harrison, B. Yao, Q. He, D. J. Morgan, F. Ni, P. Sharma, C. J. Kiely, X. Li, F. Deng, J. Xu and G. J. Hutchings, *ACS Catal.*, 2023, **13**(11), 7199–7209.
16 A. M. Zhou, J. L. Liu, B. Zhu, L. B. Di, X. S. Li and A. M. Zhu, *Plasma Processes Polym.*, 2023, **20**(6), e2200236.
17 N. K. Erfan Behravesh, Quentin Balme, Jorma Roine, Jarno Salonen, Andrey Schukarev, Jyri-Pekka Mikkola, Markus Peurla, Atte Aho, Kari Eränen, Dmitry Yu Murzin and Tapio Salmi, *J. Catal.*, 2017, **353**, 223–238.
18 M. Ousmane, L. F. Liotta, G. D. Carlo, G. Pantaleo, A. M. Venezia, G. Deganello, L. Retailleau, A. Boreave and A. Giroir-Fendler, *Appl. Catal., B*, 2011, **101**(3–4), 629–637.
19 J. Cao, Q. Guodong, B. Yao, Q. He, R. J. Lewis, X. Li, F. Deng, J. Xu and G. J. Hutchings, *ACS Catal.*, 2024, **14**, 1797–1807.
20 L. B. Di, J. Zhang, X. L. Zhang, H. Y. Wang, H. Li, Y. Q. Li and D. C. Bu, *J. Phys. D: Appl. Phys.*, 2021, **54**(11), 333001.
21 L. B. Di, J. S. Zhang and X. L. Zhang, *Plasma Processes Polym.*, 2018, **15**(5), 1700234.
22 A. M. Zhou, J. L. Liu, B. Zhu, X. S. Li and A. M. Zhu, *Chem. Eng. J.*, 2022, **433**, 134338.
23 Y. Liu, X.-S. Li, J.-L. Liu, J. Wu, D. Ye and A.-M. Zhu, *Catal. Sci. Technol.*, 2016, **6**(11), 3788–3796.
24 G. Qi, T. E. Davies, A. Nasrallah, M. A. Sainna, A. G. Howe, R. Lewis, R. J. Quesne, C. R. A. M. Catlow, D. J. Willock and Q. He, *Nat. Catal.*, 2022, **5**, 45–54.
25 M. Mihaylov, H. Knözinger, K. Hadjiivanov and B. C. Gates, *Chem. Ing. Tech.*, 2007, **79**(6), 795–806.
26 X. Q. Deng, B. Zhu, X. S. Li, J. L. Liu, X. Zhu and A. M. Zhu, *Appl. Catal., B*, 2016, **188**, 48–55.